Dynamic exchange in 3D cell culture hydrogels based on crosslinking of cyclic thiosulfinates

Janssen, M.L.; Liu, T.; Özel, M.; Bril, M.; Thelu, H.V.P.; Kieltyka R.E.

How to cite: Angew. Chem. Int. Ed. 2024, e202314738
doi.org/10.1002/anie.202314738

Hydrogels Hot Paper

Dynamic Exchange in 3D Cell Culture Hydrogels Based on Crosslinking of Cyclic Thiosulfinates

*Merel L. Janssen[+], Tingxian Liu[+], Mertcan Özel, Maaike Bril, Hari Veera Prasad Thelu, and Roxanne E. Kieltyka**

Abstract: Dynamic polymer materials are highly valued substrates for 3D cell culture due to their viscoelasticity, a time-dependent mechanical property that can be tuned to resemble the energy dissipation of native tissues. Herein, we report the coupling of a cyclic thiosulfinate, mono-*S*-oxo-4-methyl asparagusic acid, to a 4-arm PEG-OH to prepare a disulfide-based dynamic covalent hydrogel with the addition of 4-arm PEG-thiol. Ring opening of the cyclic thiosulfinate by nucleophilic substitution results in the rapid formation of a network showing a viscoelastic fluid-like behaviour and relaxation rates modulated by thiol content through thiol-disulfide exchange, whereas its viscoelastic behaviour upon application as a small molecule linear crosslinker is solid-like. Further introduction of 4-arm PEG-vinylsulfone in the network yields a hydrogel with weeks-long cell culture stability, permitting 3D culture of cell types that lack robust proliferation, such as human pluripotent stem cell-derived cardiomyocytes (hPSC-CMs). These cells display native behaviours such as cell elongation and spontaneous beating as a function of the hydrogel's mechanical properties. We demonstrate that the mode of dynamic cyclic thiosulfinate crosslinker presentation within the network can result in different stress relaxation profiles, opening the door to model tissues with disparate mechanics in 3D cell culture.

Introduction

Accurate 3D cell culture models are essential to bridge the gap with in vivo conditions to understand and treat disease. Consequently, there is a need for synthetic hydrogels that provide the biochemical and/or biophysical cues cells experience within their microenvironment in the extracellular matrix (ECM) of a given tissue.[1–5] While early synthetic polymer hydrogels aimed to steer cell behaviour by tuning network stiffness[6–8] and degradation[9,10] using covalent crosslinks between macromolecular chains, more recent hydrogel designs make use of dynamic crosslinks, such as those that are non-covalent[11–14] or dynamic covalent.[15,16] Strong yet reversible, dynamic covalent bonds permit access to complex mechanical characteristics encountered in biological tissues and ECMs, such as viscoelasticity, a time-dependent response to mechanical load involving stress relaxation.[17,18] Tissues display variable stress relaxation profiles over a large range of time scales: soft tissues like brain behave like a viscoelastic fluid, showing rapid relaxation of the applied stress and a minimal permanent elastic storage modulus, while stiffer tissues like skin or muscle appear as viscoelastic solids, reaching an equilibrium deformation and demonstrating elastic resistance at longer timescales.[17,19] Moreover, tissues can transition between fluid- and solid-like states in development and disease, for example, during gastrulation or breast cancer.[20,21] In cell culture in vitro, hydrogels that show stress relaxation can influence cellular processes such as spreading, differentiation, and morphogenesis.[18,22,23]

The selected dynamic covalent crosslinking chemistry is a critical design parameter to engineer stress relaxation in synthetic hydrogels, as the bond lifetime dictates the material response to deformation.[24–28] Their relaxation time can be tuned from seconds to hours using reactions that operate through reversible addition (e.g., in the formation of hydrazone,[29] oxime,[30,31] or boronate[32] bonds), exchange (e.g., in the formation of disulfide and thioester bonds[33,34]), or both,[35] ultimately affecting cellular response. Among these bonds, disulfides are attractive because of their biological relevance, reversibility under mild conditions, and responsiveness to various stimuli (e.g., redox, light, heat).[36–38] While networks containing disulfides enable stress relaxation through thiol- or photoinduced radical-mediated disulfide exchange,[35,37,39] they can be challenging to deploy in cell culture.[40] Air oxidation of thiols to form disulfides leads to cell sedimentation as it takes place over several hours.[41] Alternatively, oxidants such as hydrogen peroxide can increase the reaction rate but cannot be used for 3D cell encapsulation due to their cytotoxicity.[42]

Latent thiols in the form of ring-strained sulfur heterocycles offer a potent solution to overcome these 3D cell culture challenges because of their reactive character that

[*] M. L. Janssen,[+] Dr. T. Liu,[+] M. Özel, M. Bril, Dr. H. V. Prasad Thelu, Dr. R. E. Kieltyka
Department of Supramolecular and Biomaterials Chemistry, Leiden Institute of Chemistry
P.O. Box 9502, 2300 RA Leiden (The Netherlands)
E-mail: r.e.kieltyka@chem.leidenuniv.nl

[+] These authors contributed equally to this work.

can prevent the need for additional reagents to stimulate crosslinking.[43,44] Earlier work showed that covalent and supramolecular hydrogels containing a cyclic disulfide, 1,2-dithiolane (**DT**), can be triggered with light at 365 nm generating thiyl radicals to form disulfide and/or dithiolane-norbornene crosslinks using a photoinitiator. This reaction permits 3D cell encapsulation, and the resulting hydrogel stiffness, stress relaxation, and bioactivity can be tuned in space and time.[33,45,46] Although attractive, some biomedical applications may not be compatible with light-mediated crosslinking,[47–50] calling for latent strategies that do not rely on additional stimuli to form disulfides.

Cyclic thiosulfinates (**CT**) are efficient small molecule crosslinkers that yield two disulfide bonds without additional stimuli (Figure 1).[51] Mechanistically, the nucleophilic attack of a thiolate on a cyclic thiosulfinate leads to a disulfide bond and a terminal sulfenic acid that rapidly reacts with a second thiolate, forming a second disulfide in minutes. The 6-membered cyclic thiosulfinate (**6CT**) can be used as a crosslinker of 4-arm PEG-thiol (**4PEG-SH**) to prepare hydrogels for 3D cell culture.[52] Here, a short, linear crosslink between macromolecular chains is obtained, but the cyclic thiosulfinate can also yield a bifurcated crosslink if ligated to a macromolecule. Moreover, anchoring to a macromolecule can facilitate its retention under cell culture conditions as the dynamic small molecule can diffuse out of the network. Thus, we became interested in understanding the effect of altering the presentation of the dynamic crosslinker on hydrogel mechanical properties, particularly stress relaxation that is inherent to disulfide-crosslinked hydrogels and essential to mimic biological tissues in 3D cell culture.

We herein report the coupling of a cyclic 5-membered thiosulfinate, mono-*S*-oxo-4-methyl asparagusic acid (**5CT**), to polyethylene glycol (PEG) to prepare disulfide-crosslinked dynamic covalent hydrogels (Figure 1, **X % dPEG**). We examine the potential to tune the rate and extent of stress relaxation of the hydrogel network through the **5CT** presented on PEG, comparing it against the linearly crosslinked material with the small molecule **6CT**. We further use the cyclic thiosulfinate to introduce bioactivity into the materials and then evaluate these crosslinking strategies for the 3D cell culture of human pluripotent stem cell (hPSC)-derived cardiomyocytes that lack robust proliferation, examining the influence of the formed dynamic covalent networks on their behaviour.

Results and Discussion

We reacted 4-arm PEG-OH (MW = 10 kDa) with 4-methyl asparagusic acid (**DT**) or mono-*S*-oxo-4-methyl asparagusic acid (**5CT**) (Scheme S1) according to literature methods, resulting in 86 % end-functionalized **4PEG-DT** and 90 % end-functionalized **4PEG-5CT**, respectively. For **5CT**, a mixture of diastereomers (major isomer 70 %–80 %, minor isomer 30 %–20 %) obtained on oxidation[53] were coupled to the PEGs (Figure S1). Detailed synthetic procedures can be found in the Supporting Information.

We approximated the capacity of the **4PEG-5CT** macromonomer to form gel phase materials by its reaction with a 4-arm PEG-thiol (**4PEG-SH**) through vial inversion tests (Figure S2–S6). The disulfide-crosslinked hydrogels (**100 % dPEG**) formed within ca. 5 min. when the PEG concentration was higher than 6 mM (**100 % dPEG SH/5CT** 1:1,

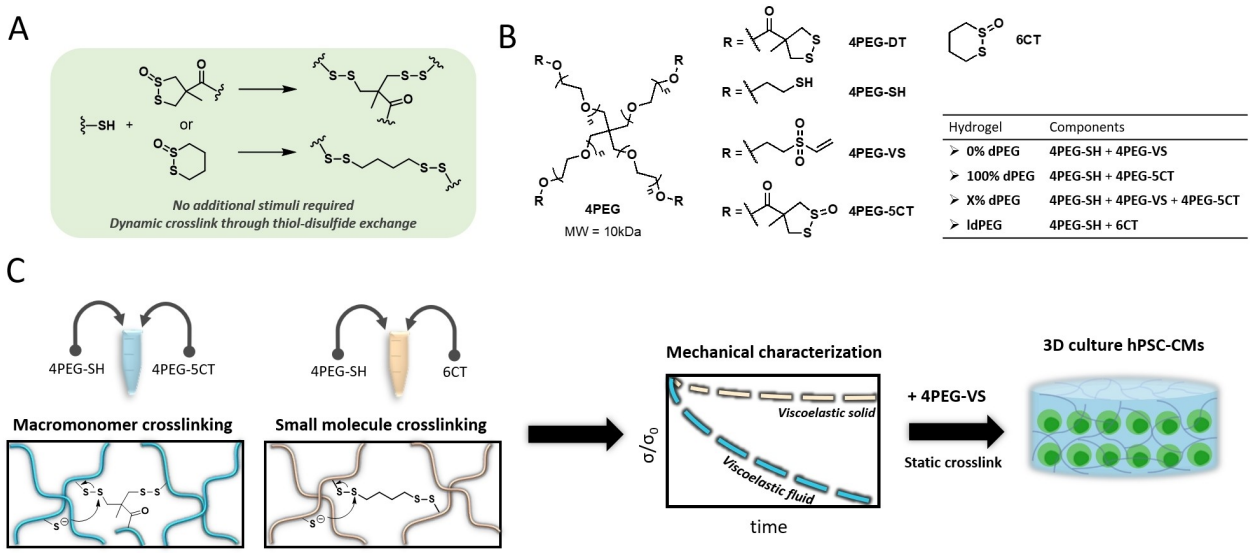

Figure 1. A) Cyclic thiosulfinates can be crosslinked using thiols without additional stimuli, yielding two disulfide bonds to form dynamic materials. (B) Components used in this study and acronyms for disulfide-crosslinked hydrogels. (C) Application of the cyclic thiosulfinate crosslinker on a macromolecule (**4PEG-5CT**) or as a small molecule (**6CT**) leads to distinct stress relaxation profiles enabled by dynamic thiol-disulfide exchange in the hydrogel networks. These crosslinking strategies are evaluated for the 3D culture of human pluripotent stem cell-derived cardiomyocytes (hPSC-CMs) that lack robust proliferation.

2:1) showcasing the rapid kinetics of the thiol/**5CT** reaction (Figure S2 and S3). We examined whether the **5CT** unit could also be used to prepare hydrogels from linear PEGs (**2PEG-5CT** and **2PEG-SH**). Hydrogelation occurred at a total macromonomer concentration of 20 mM (**2PEG-SH/2PEG-5CT** 1:1, 1:2, and 2:1) within 60 min (Figure S4), indicating the **5CT** yields a bifurcated crosslink, albeit with lower efficiency than we earlier found for 4-methyl asparagusic acid due to their distinct crosslinking mechanisms.[45] Importantly, the rapid reaction rate between thiol and **5CT** macromonomers results in fast hydrogelation, opening the door for their further biological application.

Because of their inherent reversible character, hydrogels based on exclusively dynamic covalent bonds are prone to dissolution and can be mechanically weak, requiring static or covalent crosslinks to enhance their stability for 3D cell culture.[32,54] We, therefore, used a 4-arm PEG-vinyl sulfone (**4PEG-VS**) that also reacts with **4PEG-SH** in combination with **4PEG-5CT** to prepare the gels and then performed an equilibrium swelling assay to assess their stability under cell culture conditions. We chose a thiol/**5CT** ratio of 1:1 as a starting point to retain a fraction of **5CT** for subsequent peptide coupling in later cell experiments (see below). To create three-component hydrogels, **4PEG-SH** was mixed with increasing amounts of **4PEG-VS** at the expense of **4PEG-5CT**, resulting in **X% dPEG** hydrogels, with X% indicating the relative amount of dynamic disulfide crosslinks in the material, and in contrast to hydrogels consisting exclusively of disulfide crosslinks (**100% dPEG** thiol/**5CT** 1:1 and 2:1) that dissolved within 24 h (Figure 2A), those containing **4PEG-VS** resulted in increasingly stable hydrogels (Table S1). Hydrogels containing 25% or fewer disulfide crosslinks showed comparable stability in swelling experiments to the hydrogels formed exclusively from thiol/VS crosslinks (**0% dPEG** thiol/VS 1:1, Figure S5) over 28 days, thus requiring static crosslinks to enable long-term 3D cell culture. Therefore, we selected the hydrogel containing 25% dynamic thiol/**5CT** crosslinks and 75% static thiol/VS crosslinks, **25% dPEG** (Figure S6) for subsequent studies.

We performed oscillatory rheology measurements to quantitatively assess the mechanical properties of the dynamic covalent polymer networks. For the hydrogel consisting of solely dynamic crosslinks (**100% dPEG**), higher macromonomer concentrations (4.5–8 mM) resulted in lower gelation times (from 10 min to less than 1 min) with greater stiffness (0.2 kPa–4.7 kPa) in time-sweep measurements (Figure S7). Moreover, the storage modulus (G′) increased to a greater extent when measurements were performed at 25 °C as compared to 37 °C (Figure S8), consistent with faster thiol-disulfide exchange at higher temperatures. Like **100% dPEG**, the stiffness of **25% dPEG** displayed a concentration-dependent trend in G′ increasing from 1.3 to 10.4 kPa (Figure 2B). The enhanced reactivity of **4PEG-5CT** can be observed when compared

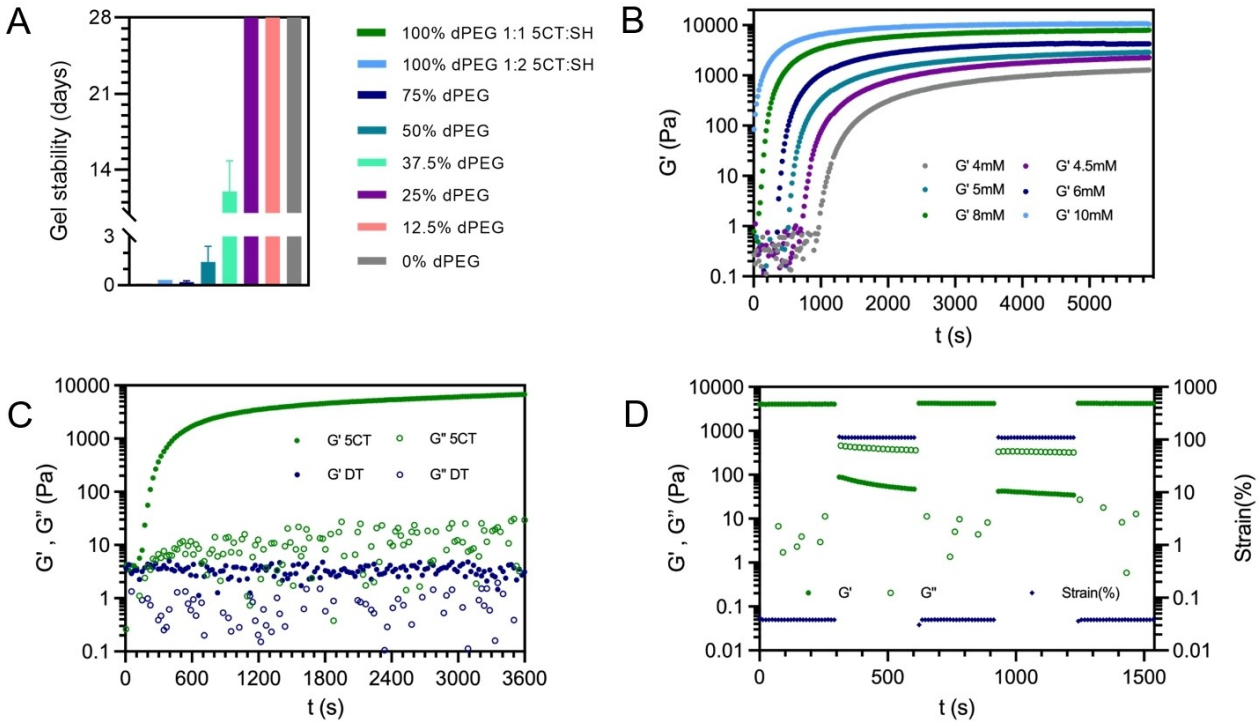

Figure 2. Oscillatory rheology and equilibrium swelling measurements: A) Equilibrium swelling measurements of **100% dPEG**, **X% dPEG**, and **0% dPEG** hydrogels (total macromonomer concentration of 6 mM) performed under cell culture conditions (37 °C, in DMEM, mean ± SD, $n = 3$). B) Time sweep measurements of **25% dPEG** hydrogels (4–10 mM) at 37 °C. C) Time sweeps of **4PEG-5CT** and **4PEG-DT** with **4PEG-SH** at 25 °C. A fixed frequency of 1 Hz and strain of 0.05% was used for all ($n = 3$). D) Step-strain experiments of **25% dPEG** (6 mM) at a frequency of 1 Hz; low (0.05%) and high strain (700%) were applied in alternation for 300s over two cycles at 37 °C.

against **4PEG-DT**, in line with earlier experiments where **5CT** was used for protein crosslinking (Figure 2C).[51] To evaluate the potential for self-recovery, we performed step-strain measurements where cycles of high (700 %) and low (0.05 %) strain were applied to **100 % dPEG** (Figure S7) and **25 % dPEG** (Figure 2D and S9) hydrogels. After applying high strain, the measured G′ returned to 90 % of its initial value for both networks, highlighting the contribution of the disulfide crosslinks even at lower percentages.

We further probed the effect of modulating the percentage of dynamic crosslinks on the stress relaxation behaviour of the materials under constant strain (Figure 3 and S10–12). We fitted the normalized stress relaxation profiles to the Kohlrausch-Williams-Watts equation (Supporting Information Equation 1),[55] which is commonly used to quantify relaxation rates in hydrogel materials to obtain β representing the distribution of relaxation time scales and a characteristic time constant (τ_k). We then used these parameters to calculate the stress relaxation half-times ($t_{1/2}$) of each material, i.e., when the stress reached half its initial value (Table S2). Hydrogels consisting solely of dynamic disulfide crosslinks (**100 % dPEG**, thiol/**5CT**) displayed a $t_{1/2}$ around 30 minutes (Figure 3A and 3B) Table S2), on the same order of magnitude as reported for other dynamic covalent chemistries.[33,56] When including static thiol/VS crosslinks at the expense of disulfides, $t_{1/2}$ can be increased to over 5 hours in **25 % dPEG** in line with the reduced percentage of dynamic crosslinks in the network. β values (Table S2) above 0.5 were found for all networks, indicating one dominant relaxation mode for the material under strain. In contrast, the total macromonomer content does not impact the rate of relaxation, indicating that the viscoelasticity of the network containing the **4PEG-5CT** depends on the dynamic covalent crosslinks (Figure S10).

To understand the influence of cyclic thiosulfinate presentation on the stress relaxation profile, we compared **100 % dPEG** against **4PEG-SH** linearly crosslinked (**ldPEG**) with the small molecule **6CT** (Scheme S2) (Figure 3C and S11). The **100 % dPEG** profile decayed continuously over the measuring period like a viscoelastic fluid. Further increasing the number of free thiols up to a ratio of 3:1 thiol/**5CT** led to a higher rate of thiol-disulfide exchange and a faster relaxing hydrogel with a $t_{1/2}$ around 30 seconds (Figure 3D). Alternatively, **ldPEG** displayed more efficient crosslinking and possessed a stress relaxation profile with a more rapid initial relaxation and reached a plateau, consistent with a viscoelastic solid.[17] Even with decreasing the amount of **6CT** relative to **4PEG-SH** to increase the amount of free thiols, the **ldPEG** largely maintained a profile with viscoelastic solid character despite an increased degree of relaxation, pointing out that the mode of dynamic cross-

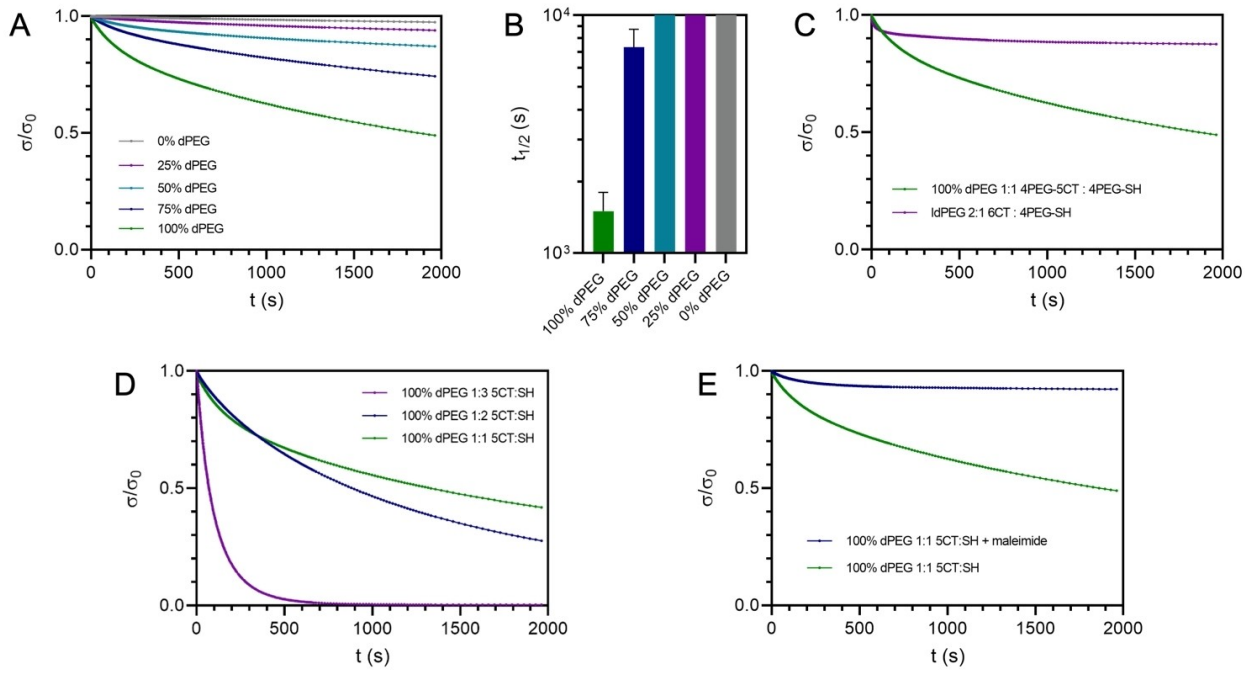

Figure 3. Stress relaxation measurements (10 % strain): A) **X % dPEG** hydrogels (6 mM) with an increasing percentage of **5CT**. B) Average $t_{1/2}$ for **X % dPEG** hydrogels, as determined by fitting data to the stretched exponential Kohlrausch-Williams-Watts equation (mean ± SD, $n = 3$). C) Comparison of **4PEG-SH** and **4PEG-5CT** (**100 % dPEG**) and **6CT** crosslinked hydrogels (**6CT-4PEG-SH**). D) Disulfide-crosslinked hydrogels (**100 % dPEG**) with increasing amounts of **4PEG-SH** relative to **4PEG-5CT**. E) Addition of a maleimide solution (6 mM) to sequester free thiols in **100 % dPEG**. All oscillatory rheology measurements were performed at 37 °C and with $n = 3$. Data is normalized to G' at 1 Hz and stress at the onset of the measurement.

linker application impacts the response of the hydrogel to constant deformation (Figure S11).

We then evaluated the contribution of dynamic thiol-disulfide exchange to the observed rheological profiles by adding a maleimide solution to react with free thiols before performing the stress relaxation test. We recorded a dramatic decrease in the extent and rate of relaxation of the **100 % dPEG** hydrogel after maleimide addition reaching a plateau within 10 minutes (Figure 3E). Similarly, relaxation was reduced to a single curve in **ldPEG** hydrogels with different thiol/**6CT** ratios (Figure S11). These results show that the free thiols are critical in both networks, and the dynamic covalent crosslinks are primarily responsible for their stress relaxation response.

Next, we sought to identify further the products generated in the thiol/**5CT** reaction that can enable dynamic exchange, and thus, tunable stress relaxation in the **X % dPEG** hydrogels. We first performed nuclear magnetic resonance (NMR) experiments reacting **5CT** with increasing amounts of a small molecule thiol, glutathione **GSH** (Figure 4A). Using an equimolar ratio, two different reaction products were detected: doubly **GSH**-substituted **5CT** (model compound, **MC1**), and the thiol-disulfide exchanged product with **GSH** (**MC2**) (Figure 4B), as well as unreacted **5CT**. The reactive sulfenic acid intermediate generated in the nucleophilic substitution reaction of **5CT** promotes the near-equivalent quantities of a doubly substituted product as previously observed in protein crosslinking,[51] and the unreacted unit at this ratio. Advantageously, the detected unreacted **5CT** can be used further introduce functionality into the dynamic covalent polymer networks as an equimolar ratio of the thiol and **5CT** macromonomers can yield gels above a certain threshold of total macromonomer content, as demonstrated above. A maximum in **MC1** of 84 % was observed when three equivalents of **GSH** to **5CT** were used. Increasing **GSH** to 8 equivalents resulted in approximately equal amounts of **MC2** and **MC1**, due to exchange of **MC1** with the excess of **GSH**. High-resolution mass spectroscopy (HR-MS) of the reaction mixture confirmed the formation of **MC1** and **MC2** observed in ^{1}H NMR (Figures S13–S17). Based on these results and earlier rheological data, we then quantified the free thiol content in the hydrogels by the Ellman's test (Figure 4C and Figure S18). Sub-millimolar amounts of free thiol were detected, increasing 7-fold from **25 % dPEG** to **100 % dPEG**, in line with larger quantity of **4PEG-5CT** that eventually gives rise to the **MC2** product. These results are also consistent with the stress relaxation data for these networks. Moreover, we also recorded a significant amount of free thiol in **0 % dPEG**. This result indicates that the incomplete reaction of thiol and vinyl sulfone macromonomers also contributes to the free thiol content measured in the various **X % dPEG** hydrogels. Importantly, the differences in free thiol content detected by the Ellman's test between the different dynamic hydrogels can be tuned and drive changes in their stress relaxation rate as measured by oscillatory rheology.

After assessing the mechanical properties of the disulfide-crosslinked materials formed from the cyclic thiosulfi-

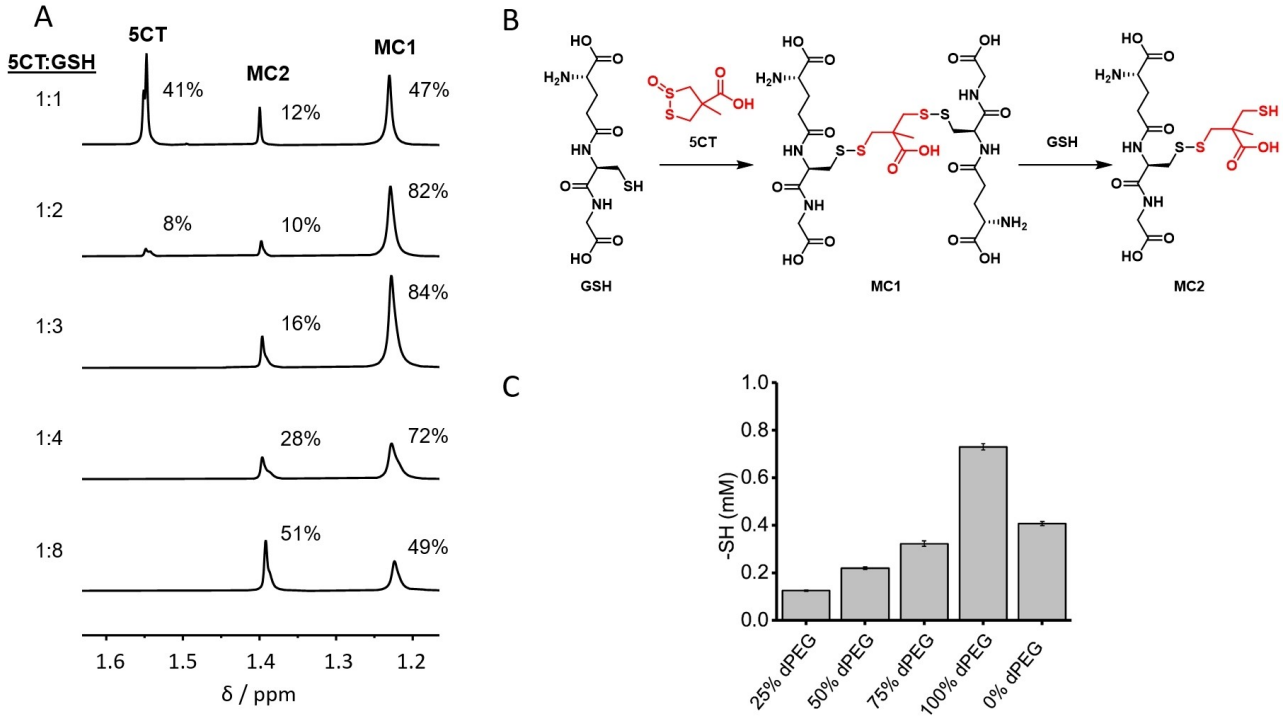

Figure 4. A) ^{1}H NMR spectra after 1 h reaction of **5CT** with increasing amounts of **GSH**, up to 8 equivalents, at 37 °C. B) HR-MS detected reaction products from the coupling of **GSH** (black) and **5CT** (red) and the proposed mechanism. C) Quantification of thiols in each hydrogel (**25 % dPEG**, **50 % dPEG**, **75 % dPEG**, **100 % dPEG**, and **0 % dPEG**) using the Ellman's test (mean ± SD, $n = 3$).

nate macromonomers and understanding their origin, we further investigated their potential for 3D cell culture. For the cells to sense the hydrogel mechanics, we ligated an RGD peptide (1 mM) with a cysteine residue at its N-terminus (**RGD-SH**) to the materials. The inclusion of the RGD peptide had no significant impact on the storage modulus or stress relaxation behaviour of the hydrogels (Figure S10). We first compared the viability of NIH3T3 fibroblasts encapsulated in the **25% dPEG** hydrogels and analogs crosslinked with 25% of small molecule **6CT** (**25% 6CT**) instead of **4PEG-5CT**. The cells remain largely viable and suspended in 3D in all hydrogels over the entire culture period (Figure S19 and S20), displaying viability over 80% in the 6 mM **25% dPEG** hydrogel and a modest decrease to 70% in **25% 6CT**. Upon further increasing the concentration of the **25% dPEG** to 10 mM, the cells stay suspended in 3D over the 4-day culture period, albeit with a 20% decrease in viability. Some cell sedimentation was also observed in the culture experiments, pointing out modification of the **25% dPEG** network by the NIH3T3 cells or media components, as the same hydrogel was found to be stable in swelling experiments in DMEM.[57,58]

We moved forward to culture human pluripotent stem cell-derived cardiomyocytes (hPSC-CMs) in the hydrogels as they are an essential tool for in vitro modeling of heart development, disease, and drug responses.[59,60] Like many soft tissues, the viscoelasticity of the cardiac extracellular matrix is important for normal cardiomyocyte function, and its relaxation rate can be altered significantly in disease.[61,62] To explore the dynamic hydrogel networks for the culture of this cell type that lacks robust proliferation, we differentiated human induced pluripotent stem cells into cardiomyocytes and seeded them in the **25% dPEG** gel to test for viability, benchmarking against **0% dPEG** and **25% 6CT**. After a 24-hour culture period, the differentiated cells showed viability above 75% for both **25% dPEG** and **0% dPEG** (Figure 5B), which is comparable to the results obtained for NIH3T3 fibroblasts. On the other hand, the viability of hPSC-CMs in the **25% dPEG-6CT** crosslinked hydrogel decreased below 50% and did not improve during the culture period, limiting the use of this network to investigate differences in stress relaxation on cell behaviour. Hence, ligation of the **5CT** crosslinking unit to a macromolecular scaffold widens the reach of this reactive unit in 3D cell culture by maintaining the viability of cell types that lack proliferative capacity.

We then studied the effect of **25% dPEG** hydrogels on hPSC-CMs behaviour over more extended culture periods using a human embryonic stem cell reporter line (double reporter *mRubyII-ACTN2* and *GFP-NKX2.5* (DRRAGN)).[63] We seeded them in the synthetic hydrogels in 3D after differentiation in 2D on Matrigel was confirmed through the expression of fluorescent cardiac markers Nkx2.5 and α-actinin, and the observation of spontaneous beating (Figure S21) on day 14. The hPSC-CMs maintained expression of cardiac markers during the culture period under all conditions (Figure S22). Using brightfield microscopy, we then captured their morphological changes over the culture period (Figure 5C and Figure S23). While hPSC-CMs exhibited a rounded morphology in **0% dPEG** (6 mM,

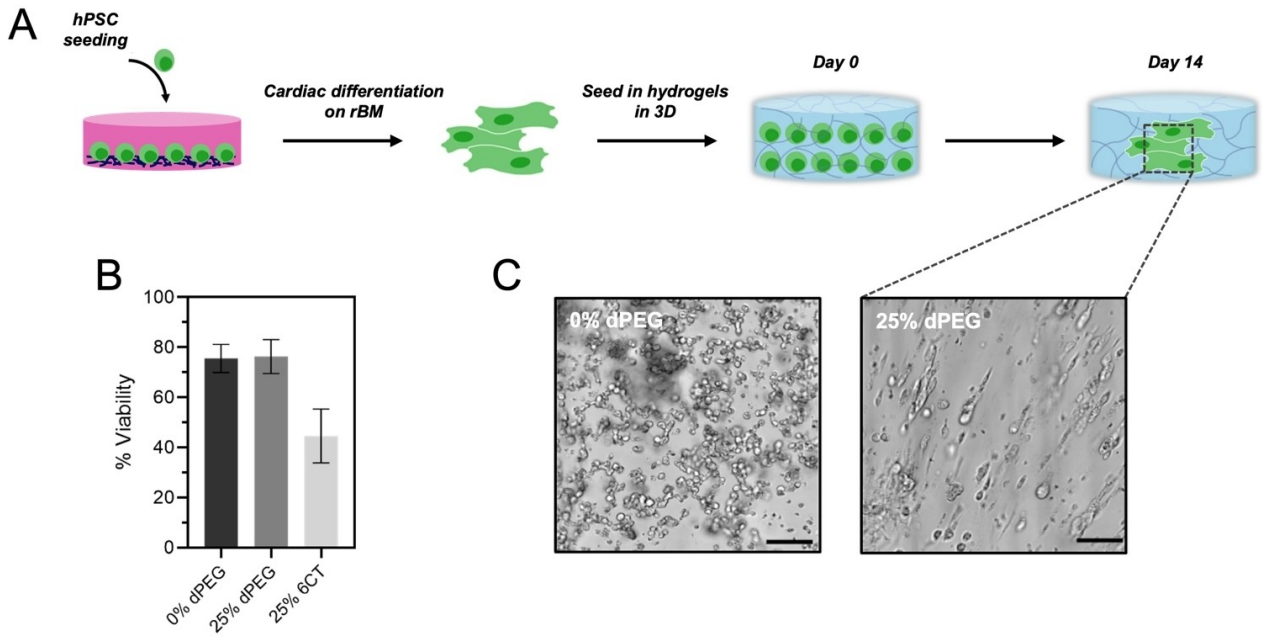

Figure 5. A) Schematic representation of hPSC cardiac differentiation, 3D encapsulation, and culture. B) Cell viability percentages of hiPSC-CMs after 24 hours of 3D cell culture in 6 mM **0% dPEG**, **25% dPEG** or **25% 6CT**-crosslinked hydrogels. Cell viability is normalized to the condition before seeding (mean ± SD, $n = 3$). C) Representative brightfield images of hESC-CMs after a 14-day culture in **0% dPEG** and **25% dPEG** hydrogels. Brightfield images are taken in a parallel z-plane to the bottom of the culture vessel. Scale bar: 100 μm.

8 kPa) hydrogels after 14 days, cells in **25% dPEG** (6 mM, 4.7 kPa) spread within 24 hours. For the stiffer hydrogel **25% dPEG** (8 mM, 8 kPa), 14 days of culture were necessary to obtain the same result. For an even stiffer gel (10 mM, 10 kPa), the hPSC-CMs presented a rounded morphology in the same period over the entire gel. In the **100% dPEG** hydrogels, the rate of stress relaxation does not depend on the total macromonomer content (Figure S10); thus, the hydrogel stiffness is likely playing a role in the delayed cell spreading in **25% dPEG** 8 mM hydrogel as compared to the 6 mM gel. Moreover, these results suggest that the crosslinking chemistry does not impede the cells from sensing the distinct mechanics of the various gels and is in line with earlier studies where cyclic 5-membered thiosulfinates were shown to be poor inhibitors of thiol-mediated uptake through integrins.[64,65] Additionally, the hPSC-CMs regained spontaneous beating after 3 days of culture in the less stiff 6 mM **25% dPEG** (Video S1), whereas we observed a delay of 10 days with its increase in 8 mM (Video S2). In the case of **0% dPEG** (6 mM, 8 kPa) that has a similar stiffness to the **25% dPEG** 8 mM hydrogel, the differentiated cells did not spontaneously beat after reseeding even after a 14-day culture period, highlighting the need for dynamic substrates to support hPSC-CM contractility in 3D.

The extent and rate of stress relaxation within synthetic matrices have been shown to be instrumental in facilitating cell spreading in 3D.[17,56] While cell responses within **25% dPEG** were observed to be on similar timescales (within 24 hours) to those with other dynamic covalent crosslinking chemistries, the stress relaxation behaviour recorded by oscillatory rheology was largely linear and only slightly different from that of the covalent **0% dPEG** network measured in PBS buffer.[66] It is envisaged that the extent and rate of stress relaxation will increase in 3D cell culture due to the presence of thiols, as previously reported for other thiol-crosslinking chemistries.[34] Our results indicate that dynamic disulfide-crosslinked hydrogels made from cyclic thiosulfinates can support native hPSC-CMs behaviours, and their tethering to a macromolecular scaffold widens their use in 3D cell culture.

Conclusion

We prepared a latent cyclic thiosulfinate macromonomer (**4PEG-5CT**) to expeditiously prepare disulfide-crosslinked dynamic covalent hydrogels by ring opening using 4-arm PEG-thiols (**4PEG-SH**). These materials show quick gelation for 3D cell encapsulation, self-recovery, and the viscoelastic behaviour needed to mimic the mechanics of tissues in the absence of additional stimuli. Compared to **4PEG-SH** crosslinked by the small molecule **6CT**, we observe significant differences in stress relaxation, transitioning from a viscoelastic fluid to a solid-like profile. This result underscores how the dynamic, bifunctional crosslinker is applied in the hydrogel network influences stress relaxation and opens new chemical space to engineer this property for in vitro tissue modeling in 3D cell culture.

While we found PEG hydrogels consisting solely of disulfide crosslinks dissolved rapidly, the introduction of **4PEG-VS** extends their application in 3D cell culture and leads to stable materials for over two weeks. Also, tuning the ratio of the various components can provide a **5CT** fraction that can be exploited to incorporate peptides for guiding cell behaviour. The **25% dPEG** hydrogel based on **4PEG-5CT** resulted in improved cytocompatibility in the 3D encapsulation of hiPSC-CMs that lack robust proliferation compared to hydrogels crosslinked by the small molecule **6CT**. Moreover, the dynamic **25% dPEG** permitted native cardiomyocyte behaviours such as contractility and spreading, in contrast to hydrogels consisting solely of static thiol/vinyl sulfone crosslinks. Notably, the cyclic thiosulfinate macromonomer strategy to prepare disulfide crosslinked hydrogels unlocks new avenues in the application space of these ring-strained sulfur heterocycles for 3D cell culture while underlining the value of dynamic covalent bonding strategies in polymer hydrogels to encourage native cell behaviours.

Supporting Information

Synthetic procedures, additional rheological data and cell culture experiments can be found in the Supporting Information.

Acknowledgements

The authors thank C. Tong for rheological measurements and R. Passier for the hPSC (DRRAGN) reporter line and essential discussions. T. Liu thanks the China Scholarship Council for her CSC scholarship. R. E. Kieltyka would like to acknowledge the European Research Council (ERC) for her ERC Starting Grant 853625—SupraCTRL.

Conflict of Interest

The authors declare no conflict of interest.

Data Availability Statement

The data that support the findings of this study are available in the supplementary material of this article.

Keywords: 3D Cell Culture · Cyclic Thiosulfinate · Dynamic Covalent Hydrogels · Stress Relaxation · Thiol-Disulfide Exchange

[1] G. Huang, F. Li, X. Zhao, Y. Ma, Y. Li, M. Lin, G. Jin, T. J. Lu, G. M. Genin, F. Xu, *Chem. Rev.* **2017**, *117*, 12764–12850.
[2] E. A. Aisenbrey, W. L. Murphy, *Nat. Rev. Mater.* **2020**, *5*, 539–551.
[3] Y. Li, E. Kumacheva, *Sci. Adv.* **2018**, *4*, eaas8998.

[4] C. M. Madl, S. C. Heilshorn, *Annu. Rev. Biomed. Eng.* **2018**, *20*, 21–47.
[5] M. Bril, S. Fredrich, N. A. Kurniawan, *Smart Mater. Med.* **2022**, *3*, 257–273.
[6] A. J. Engler, S. Sen, H. L. Sweeney, D. E. Discher, *Cell* **2006**, *126*, 677–689.
[7] M. Caiazzo, Y. Okawa, A. Ranga, A. Piersigilli, Y. Tabata, M. P. Lutolf, *Nat. Mater.* **2016**, *15*, 344–352.
[8] M. Guvendiren, J. A. Burdick, *Nat. Commun.* **2012**, *3*, 792.
[9] M. P. Lutolf, J. L. Lauer-Fields, H. G. Schmoekel, A. T. Metters, F. E. Weber, G. B. Fields, J. A. Hubbell, *Proc. Natl. Acad. Sci. USA* **2003**, *100*, 5413–5418.
[10] S. W. Hwang, C. M. Lim, C. T. Huynh, H. Moghimianavval, N. A. Kotov, E. Alsberg, A. P. Liu, *Angew. Chem. Int. Ed.* **2023**, *62*, e202308509.
[11] M. Diba, S. Spaans, S. I. S. Hendrikse, M. M. C. Bastings, M. J. G. Schotman, J. F. van Sprang, D. J. Wu, F. J. M. Hoeben, H. M. Janssen, P. Y. W. Dankers, *Adv. Mater.* **2021**, *33*, 2008111.
[12] L. Zou, A. S. Braegelman, M. J. Webber, *ACS Appl. Mater. Interfaces* **2019**, *11*, 5695–5700.
[13] T. Liu, L. van den Berk, J. A. J. Wondergem, C. Tong, M. C. Kwakernaak, B. Ter Braak, D. Heinrich, B. van de Water, R. E. Kieltyka, *Adv. Healthcare Mater.* **2021**, *10*, 2001903.
[14] S. Hafeez, F. R. Passanha, A. J. Feliciano, F. A. A. Ruiter, A. Malheiro, R. P. M. Lafleur, N. M. Matsumoto, C. van Blitterswijk, L. Moroni, P. Wieringa, V. L. S. LaPointe, M. B. Baker, *Biomater. Sci.* **2022**, *10*, 4740–4755.
[15] M. E. Smithmyer, C. C. Deng, S. E. Cassel, P. J. Levalley, B. S. Sumerlin, A. M. Kloxin, *ACS Macro Lett.* **2018**, *7*, 1105–1110.
[16] M. Rizwan, C. Ling, C. Guo, T. Liu, J.-X. Jiang, C. E. Bear, S. Ogawa, M. S. Shoichet, *Adv. Healthcare Mater.* **2022**, *11*, e2200880.
[17] O. Chaudhuri, J. Cooper-White, P. A. Janmey, D. J. Mooney, V. B. Shenoy, *Nature* **2020**, *584*, 535–546.
[18] Z. Wei, R. Schnellmann, H. C. Pruitt, S. Gerecht, *Cell Stem Cell* **2020**, *27*, 798–812.
[19] E. E. Charrier, K. Pogoda, R. G. Wells, P. A. Janmey, *Nat. Commun.* **2018**, *9*, 449.
[20] B. A. Krajina, B. L. LeSavage, J. G. Roth, A. W. Zhu, P. C. Cai, A. J. Spakowitz, S. C. Heilshorn, *Sci. Adv.* **2021**, *7*, eabe1969.
[21] E. Hannezo, C. P. Heisenberg, *Trends Cell Biol.* **2022**, *32*, 433–444.
[22] O. Chaudhuri, L. Gu, M. Darnell, D. Klumpers, S. A. Bencherif, J. C. Weaver, N. Huebsch, D. J. Mooney, *Nat. Commun.* **2015**, *6,* 6365.
[23] O. Chaudhuri, L. Gu, D. Klumpers, M. Darnell, S. A. Bencherif, J. C. Weaver, N. Huebsch, H. P. Lee, E. Lippens, G. N. Duda, D. J. Mooney, *Nat. Mater.* **2016**, *15*, 326–336.
[24] V. Yesilyurt, A. M. Ayoob, E. A. Appel, J. T. Borenstein, R. Langer, D. G. Anderson, *Adv. Mater.* **2017**, *29*, 1605947.
[25] B. Marco-Dufort, R. Iten, M. W. Tibbitt, *J. Am. Chem. Soc.* **2020**, *142*, 15371–15385.
[26] M. Rizwan, A. E. G. Baker, M. S. Shoichet, *Adv. Healthcare Mater.* **2021**, *10*, 2100234.
[27] S. Tang, B. M. Richardson, K. S. Anseth, *Prog. Mater. Sci.* **2021**, *120*, 100738.
[28] M. M. Perera, N. Ayres, *Polym. Chem.* **2020**, *11*, 1410-1423.
[29] S. Wang, G. N. Nawale, O. P. Oommen, J. Hilborn, O. P. Varghese, *Polym. Chem.* **2019**, *10*, 4322-4327.
[30] H. Sánchez-Morán, A. Ahmadi, B. Vogler, K. H. Roh, *Biomacromolecules* **2019**, *20*, 4419–4429.
[31] F. L. C. Morgan, J. Fernández-Pérez, L. Moroni, M. B. Baker, *Adv. Healthcare Mater.* **2022**, *11*, 2101576.
[32] S. Tang, H. Ma, H.-C. Tu, H.-R. Wang, P.-C. Lin, K. S. Anseth, *Adv. Sci.* **2018**, *5*, 1800638.
[33] B. R. Nelson, B. E. Kirkpatrick, C. E. Miksch, M. D. Davidson, N. P. Skillin, G. K. Hach, A. Khang, S. N. Hummel, B. D. Fairbanks, J. A. Burdick, C. N. Bowman, K. S. Anseth, *Adv. Mater.* **2023**, 2211209.
[34] T. E. Brown, B. J. Carberry, B. T. Worrell, O. Y. Dudaryeva, M. K. McBride, C. N. Bowman, K. S. Anseth, *Biomaterials* **2018**, *178*, 496–503.
[35] R. Guo, Q. Su, J. Zhang, A. Dong, C. Lin, J. Zhang, *Biomacromolecules* **2017**, *18*, 1356–1364.
[36] A. G. Orrillo, R. L. E. Furlan, *Angew. Chem. Int. Ed.* **2022**, *61*, e202201168.
[37] M. M. Perera, P. Chimala, A. Elhusain-Elnegres, P. Heaton, N. Ayres, *ACS Macro Lett.* **2020**, *9*, 1552–1557.
[38] R. Bej, P. Dey, S. Ghosh, *Soft Matter* **2020**, *16*, 11–26.
[39] Y. Deng, Q. Zhang, D. H. Qu, H. Tian, B. L. Feringa, *Angew. Chem. Int. Ed.* **2022**, *61*, e202209100.
[40] F. Goethals, D. Frank, F. Du Prez, *Prog. Polym. Sci.* **2017**, *64*, 76–113.
[41] N. Hisano, M. Noriyuki, I. Hiroo, I. Yoshito, *J. Biomed. Mater. Res.* **1998**, *40*, 115–123.
[42] Y. Sun, Y. Huang, *J. Mater. Chem. B* **2016**, *4*, 2768–2775.
[43] T. Kato, B. Lim, Y. Cheng, A. T. Pham, J. Maynard, D. Moreau, A. I. Poblador-Bahamonde, N. Sakai, S. Matile, *J. Am. Chem. Soc.* **2022**, *2*, 839–852.
[44] X. Zhang, R. M. Waymouth, *J. Am. Chem. Soc.* **2017**, *139*, 3822–3833.
[45] C. Tong, J. A. J. Wondergem, D. Heinrich, R. E. Kieltyka, *ACS Macro Lett.* **2020**, *9*, 882–888.
[46] C. Tong, J. A. J. Wondergem, M. van Den Brink, M. C. Kwakernaak, Y. Chen, M. M. R. M. Hendrix, I. K. Voets, E. H. J. Danen, S. Le Dévédec, D. Heinrich, R. E. Kieltyka, *ACS Appl. Mater. Interfaces* **2022**, *14*, 17042–17054.
[47] T. L. Rapp, C. A. DeForest, *Adv. Healthcare Mater.* **2020**, *9*, 1901553.
[48] C. G. Williams, A. N. Malik, T. K. Kim, P. N. Manson, J. H. Elisseeff, *Biomaterials* **2005**, *26*, 1211–1218.
[49] E. A. Phelps, N. O. Enemchukwu, V. F. Fiore, J. C. Sy, N. Murthy, T. A. Sulchek, T. H. Barker, A. J. García, *Adv. Mater.* **2012**, *24*, 64–70.
[50] Z. Liu, Q. Lin, Y. Sun, T. Liu, C. Bao, F. Li, L. Zhu, *Adv. Mater.* **2014**, *26*, 3912–3917.
[51] D. P. Donnelly, M. G. Dowgiallo, J. P. Salisbury, K. C. Aluri, S. Iyengar, M. Chaudhari, M. Mathew, I. Miele, J. R. Auclair, S. A. Lopez, R. Manetsch, J. N. Agar, *J. Am. Chem. Soc.* **2018**, *140*, 7377–7380.
[52] K. C. Aluri, M. A. Hossain, N. Kanetkar, B. C. Miller, M. G. Dowgiallo, D. Sivasankar, M. R. Sullivan, R. Manetsch, T. Konry, A. Ekenseair, J. N. Agar, *Bioconjugate Chem.* **2021**, *32*, 584–594.
[53] X. Marat, K. Lucet-Levannier, L. Marrot, *Administration of Dithiolane Compounds for Photoprotecting the Skin*, US8530511B2, **2013**.
[54] C. Han, H. Zhang, Y. Wu, X. He, X. Chen, *Sci. Rep.* **2020**, *10*, 14997.
[55] M. Walker, M. Godin, J. L. Harden, A. E. Pelling, *APL Bioeng.* **2020**, *4*, 036107.
[56] J. Lou, R. Stowers, S. Nam, Y. Xia, O. Chaudhuri, *Biomaterials* **2018**, *154*, 213–222.
[57] Q. Xu, C. He, Z. Zhang, K. Ren, X. Chen, *ACS Appl. Mater. Interfaces* **2016**, *8*, 30692–30702.
[58] R. K. Boz, D. Aydin, S. Kocak, B. Golba, R. Sanyal, A. Sanyal, *Bioconjugate Chem.* **2022**, *33*, 839-847.
[59] E. Giacomelli, C. L. Mummery, M. Bellin, *Cell. Mol. Life Sci.* **2017**, *74*, 3711–3739.
[60] M. T. Zhao, S. Ye, J. Su, V. Garg, *Front. Cell Dev. Biol.* **2020**, *8*, 594226.

[61] I. Andreu, T. Luque, A. Sancho, B. Pelacho, O. Iglesias-García, E. Melo, R. Farré, F. Prósper, M. R. Elizalde, D. Navajas, *Acta Biomater.* **2014**, *10*, 3235–3242.
[62] T. J. Schmeling, D. A. Hettrick, J. R. Kersten, P. S. Pagel, D. C. Warltier, *Ann. Biomed. Eng.* **1999**, *27*, 131–140.
[63] M. C. Ribeiro, R. H. Slaats, V. Schwach, J. M. Rivera-Arbelaez, L. G. J. Tertoolen, B. J. van Meer, R. Molenaar, C. L. Mummery, M. M. A. E. Claessens, R. Passier, *J. Mol. Cell. Cardiol.* **2020**, *141*, 54–64.
[64] Y. Cheng, A. T. Pham, T. Kato, B. Lim, D. Moreau, J. López-Andarias, L. Zong, N. Sakai, S. Matile, *Chem. Sci.* **2021**, *12*, 626–631.
[65] F. Coelho, S. Saidjalolov, D. Moreau, O. Thorn-Seshold, S. Matile, *JACS Au* **2023**, *3*, 1010–1016.
[66] H. Ma, L. J. Macdougall, A. Gonzalez Rodriguez, M. E. Schroeder, D. Batan, R. M. Weiss, K. S. Anseth, *Macromol. Biosci.* **2020**, *20*, 2000268.

Manuscript received: October 1, 2023
Accepted manuscript online: December 6, 2023
Version of record online: ■■, ■■

Research Articles

Hydrogels

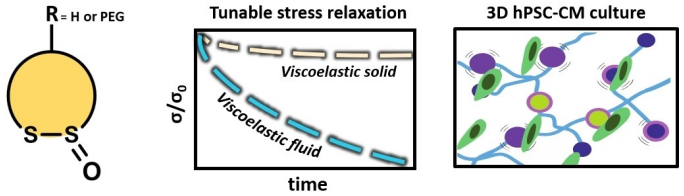

Cyclic thiosulfinates can generate disulfide-crosslinked dynamic covalent hydrogels without additional stimuli to gain control over stress relaxation based on thiol content and mode of crosslinker application. Pluripotent stem cell-derived cardiomyocytes can be 3D cultured in hydrogels containing macromonomers with this chemistry, displaying native behaviours, such as cell spreading and spontaneous beating.